Endocrine (2019) 65:252–262
https://doi.org/10.1007/s12020-019-01969-y

ORIGINAL ARTICLE

Check for updates

High dose of linagliptin induces thermogenic beige adipocytes in the subcutaneous white adipose tissue in diet-induced obese C57BL/6 mice

Byanca Ramos de Oliveira Correia[1] · Tamiris Lima Rachid[1] · Jade Sancha de Oliveira Glauser[1] · Fabiane Ferreira Martins[1] · Carlos Alberto Mandarim-de-Lacerda[1] · Vanessa Souza-Mello[1]

Received: 10 January 2019 / Accepted: 24 May 2019 / Published online: 3 June 2019

Abstract

Purpose To verify whether the treatment with linagliptin induces the browning of the subcutaneous WAT (sWAT) and thermogenesis in murine diet-induced obesity (DIO) model.

Methods Forty animals were randomly assigned to receive a control diet (C, 10% lipids as energy) or a high-fat diet (HF, 50% lipids as energy) for 10 weeks. Each group was re-divided to begin the 5-week treatment, totalizing four experimental groups: C, C-L (C plus linagliptin, 30 mg/kg body mass; BM), HF, and HF-L (HF plus linagliptin, 30 mg/kg BM). The drug was mixed with diet.

Results HF animals showed overweight, glucose intolerance, and a greater cross-sectional area of adipocytes. The treatment with linagliptin was able to normalize the BM, restore the glucose tolerance and the cross-sectional area of adipocytes. These observations comply with the observation of UCP1-positive multilocular adipocytes in the sWAT of treated animals. Both treated groups (C-L and HF-L) showed high expression of thermogenic and type 2 cytokines genes, which agree with the enhanced body temperature and the lower respiratory exchange ratio, implying enhanced thermogenesis with the use of lipids as fuel.

Conclusions The reduced BM, the enhanced body temperature, and the presence of positive UCP1 beige cells in the sWAT point to the activation of the browning cascade on the sWAT of linagliptin-treated mice, and hence, linagliptin could induce the thermogenic pathway as a pleiotropic effect that can have translational potential.

Keywords Linagliptin · Subcutaneous white adipose tissue · Browning · Obesity · Thermogenesis

Introduction

Obesity has reached epidemic proportions owing to greater availability of high energy-density foods coupled with physical inactivity [1]. The white adipose tissue (WAT) undergoes hypertrophy and hyperplasia during a chronic positive energy balance (EB), which favors the establishment of insulin resistance and inflammation [2]. These changes make obese individuals more prone to non-communicable diseases such as type 2 diabetes in the long run [3].

Recently, the concept of the WAT as a lipid reservoir has changed drastically [4]. Nowadays, the WAT is regarded as an endocrine organ, able to secrete adipokines involved with many metabolic pathways in an autocrine, paracrine, or endocrine fashion [5]. Moreover, the WAT plasticity towards a third type of adipocyte, the beige adipocyte, turned the WAT a viable target to obesity management through enhanced thermogenesis [6].

Beige adipocytes exhibit an abundant cytoplasm filled with mitochondria, where thermogenesis occurs and produces heat instead of generating adenosine triphosphate (ATP), resulting in a negative EB [7]. The browning phenomenon (beige adipocytes induction) is more frequent in the subcutaneous WAT (sWAT) and has gathered pace as it was recently estimated that the presence of 63 g of beige

✉ Vanessa Souza-Mello
souzamello.uerj@gmail.com

[1] Laboratory of Morphometry, Metabolism, and Cardiovascular Diseases, Biomedical Center, Institute of Biology, State University of Rio de Janeiro, Rio de Janeiro, Brazil

adipose tissue could avoid the storage of 4 kg of fat per year in humans [8].

Some browning agents include medicines that activate the peroxisome proliferator-activated receptor alpha (PPAR-α) [9, 10], and the angiotensin-receptor blocker losartan [11], besides some nutraceuticals that stimulate the thermogenic pathway such as cinnamon [12] or chrysin [13]. Lately, the dipeptidyl peptidase-4 (DPP-4) enzyme has been described as an adipokine, with excessive secretion in obesity, leading to insulin-resistant large adipocytes [14, 15]. Thus, the frequent use of DPP-4 inhibitors (DPP-4i) as an oral hypoglycemic agent can result in beneficial pleiotropic effects when it comes to the metabolic impairments of obesity.

In obese mice, the use of sitagliptin (DPP-4i) reduced hepatic steatosis, resulted in better preservation of the endocrine pancreas and predominance of small and insulin-sensitive white adipocytes [16]. Furthermore, linagliptin (DPP-4i) has recently been linked to enhanced PGC1α expression owing to macrophage polarization toward M2 phenotype [17]. Considering that the PGC1α is pivotal to the mitochondrial biogenesis, an essential step to the browning phenomenon [18], we carried out this study to verify whether the treatment with linagliptin induces the browning of the sWAT and thermogenesis in murine diet-induced obesity (DIO) model.

Materials and methods

Experimental design: animals and diet

Three-months-old male C57BL/6 mice were kept in pathogen-free cages, under controlled conditions of light (12/12 h dark/light cycle), temperature (21 ± 2 °C) and humidity (60 ± 10%), with free access to food and water. All procedures are in accordance with the conventional guidelines for experimentation with animals (National Institutes of Health Publication: no. 85–23, revised in 1996) and approved by the Animal Ethics Committee of State University of Rio de Janeiro (protocol CEUA 022/2018).

During 10 weeks, 40 animals were randomly assigned into two groups: 20 mice were fed a control diet (14% of energy as protein; 10% as fat and 76% as carbohydrates; total energy 15 KJ/g—C group) and the other half were submitted to a high-fat diet (14% of energy as protein; 50% as fat and 36% as carbohydrates; total energy 21 KJ/g—HF group).

After the obesity induction period, C and HF groups were re-divided, resulting in four experimental groups: Control (C, $n = 10$), Control treated with linagliptin (C-L, $n = 10$), High-fat (HF, $n = 10$), and HF treated with linagliptin (HF-L, $n = 10$). C and HF groups remained on the previous dietary scheme, whereas the treated groups had Linagliptin (Trayenta, Boehringer Ingelheim) added to the diet (manufactured by PragSolucoes–Jau, Sao Paulo, Brazil) at the dose of 30 mg/kg of BM [19]. The treatment lasted 5 weeks. All diets followed the recommendations by the AIN-93M for rodents [20].

Food intake was measured daily, and BM was measured weekly during 15 weeks of the experimental protocol.

Oral glucose tolerance test (OGTT)

In the last week of the experimental protocol, animals were submitted to the OGTT. After 6 h of food deprivation, the animals received glucose (1.0 g/kg) administrated by orogastric gavage. Blood was collected from the tail vein at 0 (baseline), 15, 30, 60, and 120 min after glucose administration and the glycemia was measured by a glucometer (Accu-Chek Performa, Roche, Sao Paulo, Brazil). The area under the curve (AUC) was calculated using the trapezoid rule (GraphPad Prism v7.03 for Windows (GraphPad Software, La Jolla CA, USA)).

Indirect calorimetry and thermography

One week before euthanasia, animals followed a 72 h protocol in the Oxylet System (Panlab/ Harvard, Barcelona, Spain), discarding the first 24 h (acclimatization time) [21]. The respiratory exchange ratio (RER) was obtained by the ratio of carbon dioxide production (VCO_2) and oxygen uptake (VO_2).

An infrared camera (FLIR C2, FLIR Systems, Wilsonville, Oregon, USA) was used for thermographic analysis—body temperature of conscious mice at room temperature were measured.

Euthanasia

After 15 weeks of protocol and 6 h of food deprivation, the animals were killed. Anesthetics ketamine (240 mg/kg) and xylazine (30 mg/kg) were injected via intraperitoneal and blood samples were obtained by cardiac puncture. The plasma was separated by centrifugation (3500 rpm, 15 min) at room temperature and stored (−80 °C).

All white fat pads (inguinal, epididymal, and retroperitoneal) were carefully dissected and weighed for calculating the adiposity index (ratio between the sum of fat pads masses and total BM) and fat distribution (intra-abdominal or subcutaneous). The interscapular brown adipose tissue (iBAT) was also harvested for histological evaluation. The subcutaneous inguinal fat pad was considered the sWAT and was stored for future analysis (in formalin to histological and immunohistochemical assays or frozen to RT-qPCR).

Plasma insulin

Plasma insulin levels were evaluated in duplicate using an ELISA Kit for rodents (Rat/Mouse Insulin ELISA kit #EZRMI-13K, Millipore, Missouri, USA).

Light microscopy and adipocyte stereology

Formalin-fixed sWAT and iBAT samples were embedded in Paraplast Plus (Sigma-Aldrich, St. Louis, MO, USA), cut with five micrometers of thickness and stained with hematoxylin and eosin for evaluation. Non-consecutive random microscopic fields were analyzed on a light microscope (Olympus BX51) using a camera (Infinity 1-5c, Lumenera Co., Ottawa, ON, Canada) and the software Image-Pro Plus (version 7.0–Media Cybernetics, Silver Spring, MD, USA).

The volume density of adipocytes in the sWAT was determined using a 16-point test frame generated by the software STEPanizer [22], as the ratio between points that hit the adipocytes (except the ones that hit the prohibited lines) and the total number of points. The numerical density of adipocyte per area was calculated by counting the adipocytes within the test frame, except the ones that cross the "forbidden lines". The average cross-sectional area of the adipocytes was estimated by stereology as the ratio between the volume density of adipocytes and twice the numerical density of adipocytes per area [23].

UCP1 immunofluorescence

After the steps of deparaffinization, antigen retrieval (performed with citrate buffer ph 6.0), nonspecific blockade and binding (ammonium chloride and glycine 2% and 5% bovine serum albumin in phosphate-buffered saline), sWAT samples (5μm-thick) were incubated with anti-UCP1 (anti-goat, SC-6529, Santa Cruz Biotechnology; 1:50 dilution) as primary antibody. Anti-goat Alexa Fluor 488 conjugate was used as the secondary antibody. Slow fade (Invitrogen, Molecular Probes, Carlsbad, CA, USA) was used to mount the slides and to maintain fluorescence. A fluorescence microscope (Nikon Confocal Laser Scanning Microscopy–Model C2; Nikon Instruments, Inc., New York, EUA) was used to assess the slides.

qPCR

Levels of mRNA in the sWAT were measured through qPCR as previously described [9], using a StepOne plus Cycler and the SYBR Green mix (Invitrogen). Primers were designed using Primer3online software (version 4.0.0): Peroxisome proliferator-activated receptor alpha (*Ppar-α*—FW: CAAGGCCTCAGGGTACCACTAC; RV: GCCGA ATAGTTCGCCGAAA); Peroxisome proliferator-activated receptor Gamma Coactivator 1 alpha (*Pgc1α*—FW: AAC-CACACCCACAGGATCAGA; RV: TCTTCGCTTTATT GCTCCATGA); PR Domain-containing protein 16 (*Prdm16*—FW: AGGGCAAGAACCATTACACG; RV: GGAGGGTTTTGTCTTGTCCA); Beta3-Adrenoreceptor (*β3-ar*—FW: ACAGGAATGCCACTCCAATC; RV: AAG GAGACGGAGGAGGAGAG); Uncoupling Protein 1 (*Ucp1*—FW: TCTCAGCCGGCTTAATGACT; RV: TGCATTCTGACCTTCACGAC); Cluster of differentiation 68 (*Cd68*—FW: CCAATTCAGGGTGGAAGAAA; RV: ATGGGTACCGTCACAACCTC); Interleukin-5 (*Il-5*—FW: CACCAGCTATGCATTGGAGA; RV: TCCTCGCCACACTTCTCTTT); Interleukin-9 (*Il-9*—FW: CCTTGCCTCTGTTTTGCTCT; RV: CCTTGCCTCTGT TTTGCTCT); Interleukin-13 (*Il-13*—FW: CTGGA TTCCCTGACCAACAT; RV: GGTTACAGAGGCCAT GCAAT); and *Beta-actin*.

The beta-actin gene was used as an endogenous control to normalize selected gene expression. Efficiencies of qPCR for the target gene and the endogenous control were approximately equal and were calculated from a cDNA dilution series. The relative mRNA expression ratio (RQ) was calculated using the equation $2^{-\Delta\Delta}C_t$, in which $-\Delta\Delta C_t$ refers to the difference between the number of cycles (C_t) of the target genes and the endogenous control. Gene and protein symbols were standardized [24]. The gene symbols are italicized, with the first letter capitalized. Protein symbols are the same as the gene symbol, but in uppercase.

Data analysis

Values are expressed as the means and standard deviation. Normal distribution and homoscedasticity of variances were confirmed, we used the *t* test (during the period of two experimental groups) and analysis of variance (ANOVA) followed by Holm–Sidak post hoc test (treatment phase). Also, the two-way ANOVA was used to evaluate the contribution of each variable (diet and treatment), as well as possible interactions regarding the endpoints being assessed (GraphPad Prism v7.03 for Windows (GraphPad Software, La Jolla CA, USA). In all cases, P value < 0.05 was accepted as statistically significant.

Results

Food behavior and body mass

The higher energetic density of the HF diet reflected in the BM and adiposity index of the animals. C (means = 25.42 g) and HF (means = 25.56 g) groups started the protocol with no difference regarding the BM. After 2 weeks of ingestion of their diet, the HF group showed a higher BM

than the C group (+7%, $P = 0.0396$). This difference regarding BM lasted until the end of the experiment (15th week, +17%, $P = 0.0037$). The treatment began to affect the BM on the 13th week (third week of Linagliptin administration): HF-L group had a BM reduction in comparison with HF (−9%, $P = 0.0356$) and it also lasted until the end of the experiment (Fig. 1a). There was no difference regarding the average weekly food intake, in grams, between the groups throughout the 15-week-protocol (Table 1), despite the highest energy intake in

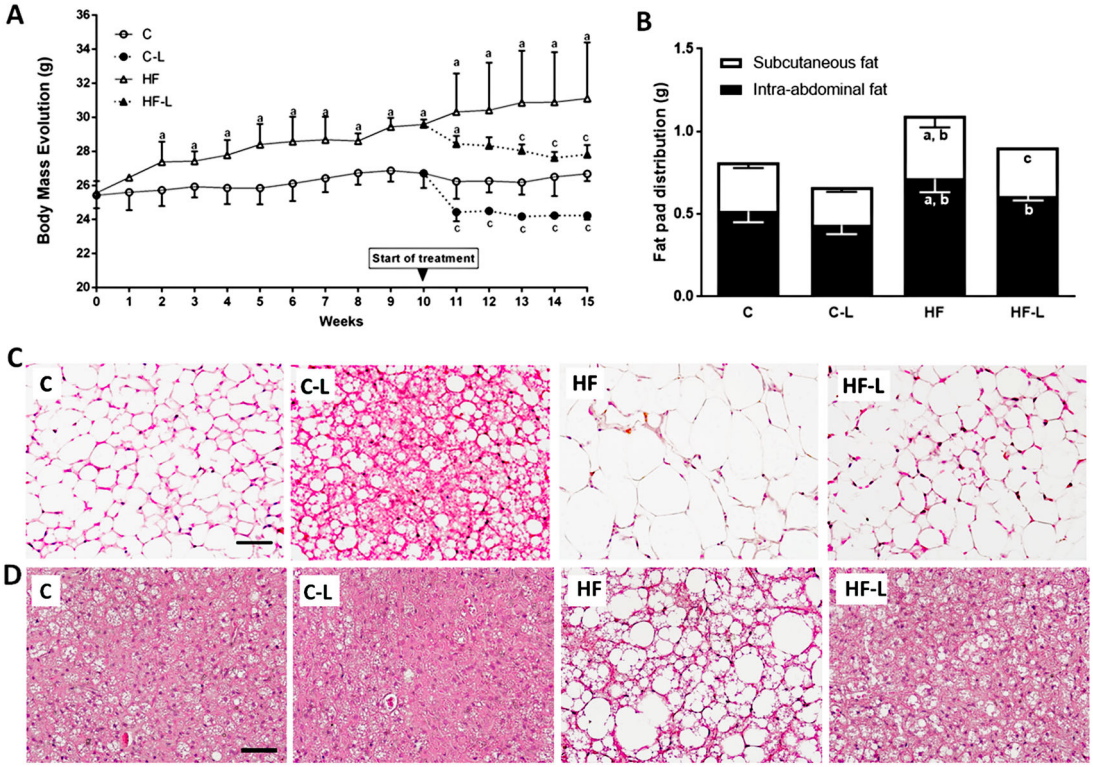

Fig. 1 Weekly body mass evolution **a**, fat pad distribution **b**, subcutaneous white adipose tissue histology **c**, and brown adipose tissue morphology **d**. Photomicrographs of subcutaneous white adipose tissue and interscapular brown adipose tissue stained with hematoxylin-eosin (same magnification to all images, bar = 50 µm). One-way ANOVA and Holm–Sidak post hoc test (mean ± SD, $n = 10$). Significant differences ($P < 0.05$) are indicated: a ≠ C; b ≠ C-L; c ≠ HF. Group abbreviations: C (control), C-L (control diet plus linagliptin), HF (high-fat), HF-L (high-fat diet plus linagliptin)

Table 1 Food behavior, adiposity, insulinemia, and energy metabolism

Data	C	C–L	HF	HF–L
Initial body mass (g) $n = 10$	26.71 ± 0.861	–	29.58 ± 0.296[a]	–
Final body mass (g) $n = 5$	26.68 ± 0.420	24.13 ± 0.233	31.11 ± 3.283[a,b]	27.82 ± 0.543[b,c]
Adiposity index (%) $n = 5$	3.454 ± 0.270	3.297 ± 0.495	4.528 ± 0.810[a,b]	3.403 ± 0.144[c]
BAT mass (g) $n = 5$	0.079 ± 0.008	0.112 ± 0.007[a]	0.110 ± 0.029[a]	0.102 ± 0.003
Body temperature (°C) $n = 10$	33.81 ± 0.716	35.04 ± 0.503[a]	34.32 ± 0.522[b]	35.04 ± 0.455[a,c]
sWAT adipocytes area (µm²) $n = 22$	60.6 ± 22.22	48.06 ± 12.02	97,39 ± 28.15[a,b]	46.26 ± 7.33[a,c]
Energy intake (KJ/day/animal) $n = 10$	39.450 ± 0.711	39.650 ± 0.196	51.470 ± 0.705[a,b]	51.740 ± 0.807[a,b]
Food intake (g/day/animal) $n = 10$	2.484 ± 0.045	2.493 ± 0.020	2.447 ± 0.050	2.443 ± 0.064
Plasma Insulin (pg/mL) $n = 5$	1409.00 ± 290.50	1155.00 ± 243.40	2210.00 ± 385.10[a,b]	1922.00 ± 464.30[b]
O_2 consumption (VO2) $n = 5$	22.10 ± 1.928	24.36 ± 1.964	24.24 ± 2.091	25.10 ± 1.479
CO_2 production (VCO2) $n = 5$	21.66 ± 1.854	21.88 ± 1.223	21.76 ± 2.022	17.06 ± 2.004[a,b,c]
Respiratory exchange ratio (RER) $n = 5$	0.981 ± 0.001	0.900 ± 0.040[a]	0.898 ± 0.030[a]	0.678 ± 0.040[a,b,c]

Data presented as the means ± SD. Significant differences ($P < 0.05$) are indicated: a ≠ C; b ≠ C-L; c ≠ HF as determined by one-way ANOVA and Holm–Sidak post hoc test for all parameters, except for initial body mass that was tested with Student's *t* test

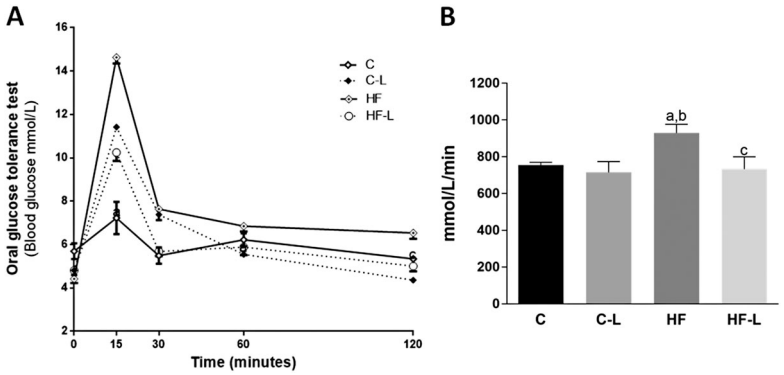

Fig. 2 Oral glucose tolerance test curve **a** and area under the curve **b**. One-way ANOVA and Holm–Sidak post hoc test (mean ± SD, $n = 5$). Significant differences ($P < 0.05$) are shown: a ≠ C; b ≠ C-L; c ≠ HF. Group abbreviations: C (control), C-L (control diet plus linagliptin), HF (high-fat), HF-L (high-fat diet plus linagliptin)

the groups fed the HF diet in comparison with the ones fed the C diet.

Adiposity index and fat distribution

Adiposity index revealed that the HF group had a significant increase on adiposity percentage relative to BM when compared with other groups (+33%, +31%, and +37% than HF-L, C e C-L, respectively; $P < 0.05$, Table 1). It is essential to highlight that the HF-L group exhibited a marked decrease in the adiposity index in comparison with the HF group (−25%, $P = 0.0128$, Table 1).

The fat distribution between the different compartments showed that the HF group had a higher mass of subcutaneous fat than C (+30%, $P = 0.0194$), C-L (+69%, $P < 0.0001$) e HF-L (+30%, $P = 0.0194$, Fig. 1b) groups. Concerning the intra-abdominal fat, C and C-L had smaller depots than HF group (−27% to C group, $P = 0.0006$ and −39% to C-L group, $P < 0.0001$). Interestingly, HF-L group had a similar intra-abdominal fat mass to C group (Fig. 1b).

Regarding the iBAT mass, HF and C-L groups showed higher masses than the C group (+39%, $P = 0.0294$ and 42%, $P = 0.0239$, respectively), whereas the HF-L group showed no difference in comparison with the C group (Table 1).

sWAT morphology and stereology

Histological images and stereological analysis reinforce the previous results. Photomicrographs of the C group showed normal-sized unilocular white adipocytes, while the HF group shows enlarged unilocular adipocytes (Fig. 1c). Both treated groups showed unilocular white adipocytes comparable to the C group, besides browning depots characterized by multilocular adipocytes. The cross-sectional area of sWAT adipocytes was significantly higher in the HF group when compared to C and C-L groups (+38% and +51%, respectively; $P < 0.0001$), confirming the hypertrophy of adipocytes and, therefore, the correct induction of obesity. HF-L group presented with a significant decrease of this parameter when compared with HF (−52.5%, $P < 0.0001$) and C groups (−24%, $P = 0.038$), indicating a considerable reduction on fat accumulation within the adipocytes, which may be related to its thermogenic capacity (Table 1).

OGTT and plasmatic insulin

After glucose administration, all groups showed a glycemic peak at 15 min. Both treated groups reestablish initial glycemia (T0) after 30 min; C group reached the T0-glycemia near 60 min after the glucose overload, whereas HF group could not grasp the former parameter during the experiment time (Fig. 2a). The AUC analysis (Fig. 2b) showed the HF group with the highest AUC when compared with all other groups (+27%, +23%, and +30% than HF-L, C e C-L groups, respectively; $P < 0.001$). There was no difference regarding AUC among C, C-L and HF-L group. This fact suggests that linagliptin tackled the oral glucose intolerance in HF-L group. Plasma insulin levels agree with the oral glucose intolerance in HF group: +57%, $P = 0.0139$ in comparison with C group and +91% in comparison with the C-L group, $P = 0.0016$, respectively; Table 1; HL-F had a lower level of plasma insulin than HF but was not significant.

iBAT morphology, indirect calorimetry, thermography, and immunofluorescence

iBAT photomicrographs showed that HF animals had multilocular brown adipocytes with larger lipid droplets than the other groups, suggesting the whitening phenomenon (Fig. 1d). Importantly, the HF-L iBAT resembled the cytoarchitecture of C and C-L groups, implying that a higher metabolism through thermogenesis was induced by the linagliptin treatment (Fig. 1d). Accordingly, the indirect calorimetry showed that the O_2 consumption did not differ among the groups, but the CO_2 production was lower in the HF-L group than in all the other groups (HF-L was 21% lower than C group, $P = 0.0039$, and 22% lower than C-L

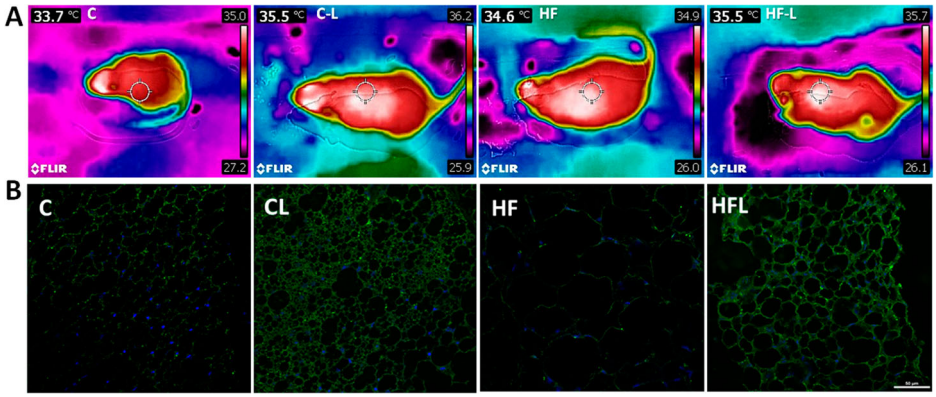

Fig. 3 Dorsal view of infrared thermography at the end of the treatment **a** and immunofluorescence for UCP1 in the subcutaneous white adipose tissue **b**. **a** The Infrared thermography shows body temperature of animals at the top left of each photograph, being the white and red areas the warmest ones. **b** A fluorescent dye was conjugated to the secondary antibody for UCP1 immunostaining in the sWAT, calibration bar = 50 µm. Group abbreviations: C (control), C-L (control diet plus linagliptin), HF (high-fat), HF-L (high-fat diet plus linagliptin)

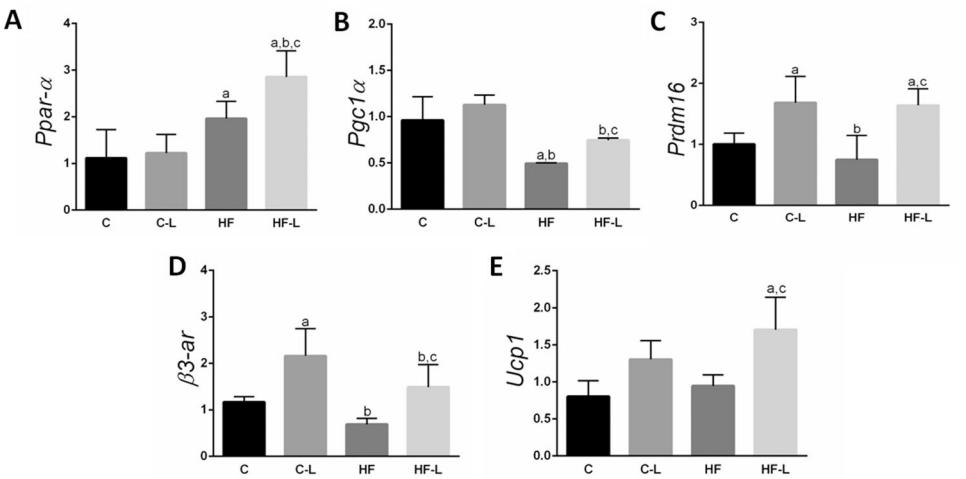

Fig. 4 Subcutaneous white adipose tissue thermogenic markers. One-way ANOVA and Holm–Sidak post hoc test (mean ± SD, $n = 5$). Significant differences ($P < 0.05$) are indicated: a ≠ C; b ≠ C-L; c ≠ HF. Group abbreviations: C (control), C-L (control diet plus linagliptin), HF (high-fat), HF-L (high-fat diet plus linagliptin)

and HF groups, $P = 0.0041$, Table 1), resulting in a reduced RER. The C group reached a higher RER than all the other groups; HF-L had the lowest RER. Meanwhile, C-L and HF had intermediate results (HF-L was 31% lower than C group, 25% lower than C-L and 24% lower than HF; $P < 0.0001$; Table 1).

The average body temperature of treated animals was higher than their respective non-treated counterparts: C-L increased in comparison with C group (+4%; $P < 0.0001$) and HF-L increased in contrast to HF group (+2%; $P = 0.221$; Table 1 and Fig. 3a). Immunofluorescence for UCP1, the critical protein for thermogenetic activity, revealed positive protein expression in both treated groups, corroborating the initial findings (Fig. 3b).

Gene expression—thermogenic markers

qPCR results (Fig. 4) showed that mRNA relative expression of *Ppar-α* (Fig. 4a), a transcription factor that has thermogenic markers as target genes, was higher in HF-L group than in all other groups (+45% than HF, $P = 0.0451$, +133% than C-L, $P = 0.0004$ and +155% than C, $P = 0.0002$).

The thermogenic marker and master regulator of mitochondrial biogenesis *Pgc1α* (Fig. 4b) has significantly enhanced expression in HF-L when compared with the HF group: +51% on HF-L ($P = 0.0331$). C and C-L groups did not show significant differences between them. *Prdm16* (Fig. 4c), a pivotal gene to the maintenance of the beige phenotype in the adipose tissue, showed higher expression in both treated groups: C-L was 68% higher than C ($P = 0.0212$), and HF-L was 118% higher than HF ($P = 0.0034$). Of note, HF-L had a 63% increase in the expression of *Prdm16* when compared with the C group ($P = 0.0249$).

Similarly, the relative expression of *β3-ar* mRNA showed higher levels in treated groups, indicating that the thermogenic pathway must be activated (Fig. 4d). HF-L had 117% more expression than HF ($P = 0.0198$), and C-L had 85% more expression than C ($P = 0.0050$).

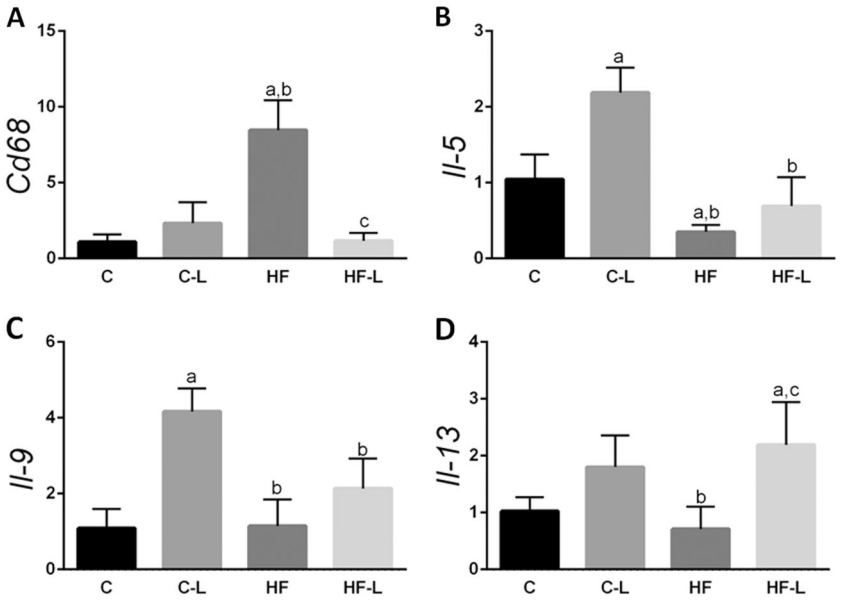

Fig. 5 Subcutaneous white adipose tissue inflammatory markers. One-way ANOVA and Holm–Sidak post hoc test (mean ± SD, $n = 5$). Significant differences ($P < 0.05$) are indicated: a ≠ C; b ≠ C-L; c ≠ HF. Group abbreviations: C (control), C-L (control diet plus linagliptin), HF (high-fat), HF-L (high-fat diet plus linagliptin)

The relative expression of *Ucp1* (Fig. 4e) corroborates the previous data: treated groups had elevated expression in comparison to their non-treated counterparts, but only HF-L had significantly higher levels than HF (+80%, $P = 0.0032$). HF-L also showed a significant difference to the C group (+112%, $P < 0.0008$).

Gene expression—inflammatory markers

The gene expression of *Cd68* (M1 macrophage marker), showed that the HF group presented with higher gene expression than C and C-L groups (+675%; $P < 0.0001$ and +263%; $P < 0.0001$, respectively). In contrast, the HF-L group had its expression markedly reduced when compared with the HF group (−86%, $P < 0.0001$), indicating that pro-inflammatory pathways were probably less activated in this treated group (Fig. 5a).

These observations regarding the *Cd68* expression complies with the *Il-5*, IL-9, and IL-13 gene expression, cytokines related to anti-inflammatory characteristics. The lowest *Il-5* gene levels were found in the HF group, with statistically significant differences in comparison to C and C-L groups (−64%; $P = 0.0068$ and − 84%; $P < 0.0001$). Conversely, linagliptin seemed to restore the *Il-5* gene expression in the HF-L group, which did not show the difference when compared with the C group (Fig. 5b). Regarding *Il-9* expression, both treated groups presented raised values concerning non-treated counterparts, but only the C-L group showed a significant difference in comparison with the C group (+282%, $P = 0.001$, Fig. 5c). A similar pattern was observed on *Il-13* expression: both treated groups presented with enhanced levels of the marker, but only the HF-L had a significantly higher *Il-13* expression than the HF group (+208%, $P = 0.0052$, Fig. 5d).

Two-way ANOVA

The diet, as a single factor, exerted the most potent effect on BM ($P < 0.0001$, accounting for 47% of the total variance), energy intake ($P < 0.0001$, accounting for 98% of total variance), abdominal fat pad ($P < 0.0001$, accounting for 62% of total variance), insulin levels ($P = 0.0002$, accounting for 56% of total variance), *Ppar-α* and *Pgc1α* expression ($P < 0.0001$, accounting for 62% of the total variance for both genes), and *Il-5* expression ($P < 0.0001$, accounting for 55% of the total variance).

The linagliptin treatment, as a single factor, exerted the most potent effect on adiposity index ($P = 0.0110$, accounting for 23% of the total variance), average adipocyte cross-sectional area ($P = 0.0016$, accounting for 36% of the total variance), AUC of the OGTT ($P = 0.0001$, accounting for 37% of the total variance), body temperature ($P < 0.0001$, accounting for 43% of the total variance), *Prdm16* expression ($P < 0.0001$, accounting for 61% of the total variance), *β3-ar* expression ($P < 0.0001$, accounting for 49% of the total variance), *Ucp1* expression ($P < 0.0001$, accounting for 50% of the total variance), *Il-9* gene expression ($P < 0.0001$, accounting for 55% of the total variance), and *Il-13* expression ($P = 0.0002$, accounting for 56% of the total variance).

The diet and the treatment, as single factors, influenced equally the subcutaneous fat pad values ($P = 0.0007$, 34% of the total variance attributed to each factor).

Diet and treatment interacted significantly regarding adiposity index ($P = 0.0453$), iBAT mass ($P = 0.0079$),

average adipocyte cross-sectional area ($P = 0.0348$), AUC of the OGTT ($P = 0.0036$), CO_2 production ($P = 0.0021$), RER ($P = 0.0002$), and *Cd68* expression ($P < 0.0001$).

Discussion

Linagliptin at the dose used and in this DIO mouse model was able to restore BM, adiposity index, and insulin resistance to values similar to the control group. These significant metabolic outcomes can be accounted for by an apparent tackling of the iBAT whitening parallel to the browning of the sWAT after the treatment with linagliptin. The browning phenomenon is supported by the augmented expression of *Ppar-α* and anti-inflammatory type 2 cytokines, leading to favored expression of thermogenic markers, positive UCP1 immunostaining and enhanced body temperature in DIO mice treated with linagliptin.

Reduction of BM started after 3 weeks of the drug administration and can be confirmed by the decrease in adiposity index and change in the morphology of the sWAT —a drop on the cross-sectional area of sWAT adipocytes implies diminished lipid depots. As there was no difference in food intake and there was a similarity in energy intake between HF-L and HF groups, the BM reduction observed herein can be accounted for by the treatment. The food behavior was compatible with a previous study using the same dose [19].

Linagliptin acts in carbohydrate metabolism, is indicated for patients with type 2 diabetes mellitus. The mechanism of action goes through the inhibition of the enzyme and adipokine DPP-4, which inactivates intestinal incretin hormones (as GIP and GLP-1). DDP-4 inhibition promotes an increased pancreatic secretion of postprandial insulin owing to prolonged action of the incretins [25]. Hence, glucose control of insulin-resistant patients could be improved [26]. Linagliptin action is glucose-dependent, and, therefore, it presents a low risk of hypoglycemia events [25–27].

Analysis of OGTT and its respective AUC showed that the animals exposed to the insult of the HF diet had difficulty in re-establishing the initial glycemia throughout the test. This result agrees to the hyperinsulinemia found in the HF group. Linagliptin restored the glucose tolerance in HF-L group, which did not present difference in comparison with the C group. On the contrary, the insulin levels did not change significantly in the HF-L group and this can be explained by the augmented half-life of incretins promoted by DDP-4 inhibition, which yields a higher release of insulin, and accordingly, higher plasma insulin levels - the drug can keep >80% of inhibition of DDP-4 during 24 h in humans [19].

Light microscopy images revealed browning depots on sWAT of treated animals. The photomicrographs show multilocular adipocytes dispersed within the unilocular white adipocytes and these depots are more visible in the C-L group. Though the drug effect on carbohydrate homeostasis is glucose-dependent, it is probable that its pleiotropic effects are not as lean animals benefited from the treatment as well. Both treated groups presented structural changes in sWAT morphology, in different intensities, in this study. These observations comply with the reduced BM observed in treating animals once excessive fat intake might be used as fuel to the enhanced thermogenesis instead of being stored [6].

Evidence for enhanced thermogenesis also came from the analysis of the iBAT photomicrographs. The HF group showed large lipid droplets within the brown adipocytes, which is not usual. This observation is suggestive of the whitening phenomenon, which is triggered by reduced vascularization and pro-inflammatory signals that turn the brown adipocyte into a white-like adipocyte, compromising its thermogenic capacity [28, 29]. Conversely, the HF-L group showed multilocular adipocytes in the iBAT resembling the cytoarchitecture of the C group, being suggestive of a standard thermogenesis capacity, which indeed helped to the BM reduction and the amelioration of the glucose homeostasis found after the treatment.

As for the fuel to the thermogenesis, the RER indicates the preferred energy source to maintain the basal metabolism of animals. HF-L had the lowest ratio between carbon dioxide production and oxygen consumption (close to 0.7) and that indicates that lipids were the primary energy source to maintain the body reactions of those animals; C group, on the other hand, presented a ratio that means carbohydrate consumption (close to 1.0) [30]. Increased body temperature on both treated groups suggests that the reduction of BM could have happened by the loss of energy as heat (thermogenesis), using lipids as substrate.

Immunofluorescence images and qPCR confirmed the previous findings. Immunostaining for UCP1, located on the inner mitochondrial membrane, showed positive immunoreactions to the protein, which is the thermogenesis effector. The thermogenic cascade starts through adrenergic stimulation [31], which triggers the elevation of the cyclic AMP and the activation of protein kinase A, which induces lipolysis. The free fatty acids activate UCP1, which allows H^+ protons to return from the intermembrane space, avoiding the ATP formation, its consequent accumulation, and enabling energy to be released as heat [32–34]. At the temperature that this study was carried out, the increased expression of UCP1 in the sWAT indicates browning because only low temperatures (4 °C) could induce browning in the sWAT. Herein, the evidence of UCP1-positive cells in the sWAT confirms these cells as beige adipocytes [35]. Also, the expression of *β3-ar* was influenced only by treatment and showed the trigger to start the thermogenic pathway in both treated groups [36].

PPAR-α, a critical transcription factor that has thermogenic markers as targets, presents basal levels in rodents [37]. PPAR-α agonists can be used as anti-obesogenic drugs [38], with potential effects on thermogenesis and browning phenomenon [10]. HF-L group presented the highest expression of this marker among all groups, which was influenced mainly by the treatment. Hence, we propose a possible interaction between DPP-4 inhibition and PPAR-α activation, which paves the way for a more detailed exploration of this interaction in further studies.

One of the PPAR-α target gene is PGC1α, considered a pivotal marker to mitochondrial biogenesis [34] and an activator of UCP1 transcription [31]. HF-L group showed higher expression of *Pgc1α* than the HF group, which can be considered as a restoration of its levels considering that HF-L values were like C group. The higher level of *Ppar-α* can explain this observation owing to a possible pleiotropic action of linagliptin as a PPAR-α agonist. Moreover, it is established that the DPP-4 inhibition promotes macrophage polarization on WAT to the M2 status [17] that are related to anti-inflammatory signaling, transcription of β-oxidation factors and an increase of PGC1α through the NF-kB inhibition [39]. In agreement to this, the sWAT of HF animals showed higher *Cd68* expression, a surface marker of macrophage [40]. Positive CD68 macrophage is a common finding in the adipose tissue of obese and diabetic subjects [41], which is linked to the obesity lipotoxicity. It can be argued that linagliptin rescued the macrophage infiltration in the sWAT as the HF-L group showed a *Cd68* expression similar to the C group.

Adaptive thermogenesis, characterized by the extra heat production, can be induced by cold, food intake, or exercise [33, 34], and white adipocytes are more sensitive to this phenomenon. Under stimulation, the white adipocyte acquires the phenotype of brown adipocytes linked with a high mitochondrial density (and therefore a higher thermogenic capacity) and morphological change in the lipid droplet (that becomes multilocular) occur [31]. The resulting beige phenotype cannot be maintained without enhanced PRDM16 levels [31, 42], whose ablation makes the beige cells return to its white phenotype, with a single lipid droplet, low mitochondrial density and low UCP1 [34]. The augmented levels of *Prdm16* expression found in treating animals reinforces that beige phenotype the linagliptin-induced beige cells were being sustained.

The browning phenomenon relies on adequate sympathetic stimulation. In this context, there is growing evidence that the sWAT maintains its adrenergic tone through a hematopoietic circuit that consists of eosinophils and alternatively activated macrophages (M2) [43]. A recent study showed that the activation of group 2 innate lymphoid cells (ILC2s) by IL-33 administration led to beige adipocyte recruitment in the sWAT of mice on the basis that the high secretion of IL-5 and IL-13 (type 2 cytokines) stimulates the proliferation of PDGFRα + adipocyte precursor cells, which are committed to differentiate into a beige adipocyte [44]. Herein, we showed that both treated groups presented high expression of *Il-5* and *Il-13* coupled with high sympathetic tone through enhanced *β3-ar* expression. These observations comply with the beige adipocyte recruitment observed in both groups and suggest a possible role of linagliptin on the IL-33/ILC2s axis and the following favored type 2 cytokines release (IL-5 and IL-13), as a new and promising target to obesity control in both human and mice through UCP1 induction in beige adipocytes and energy homeostasis [45].

It is noteworthy to say that the HF-L group showed higher *Ucp1* expression than C and HF groups, implying a higher content of active mitochondria. This result, coupled with the high *Prdm16* expression, the highest *Ppar-α* expression among all the groups, increased body temperature and the observation of the histological images led us to believe that the browning phenomenon must have occurred at different times in the treated groups. C-L must have had the thermogenic pathway activated earlier, whereas the HF-L group had to deal with the HF diet insult in the first place, and at the end of the experiment was expressing the markers of thermogenesis more actively.

The main findings of this study are depicted in Fig. 6. In brief, linagliptin-induced type 2 cytokines secretion (IL-5 and IL-13) in the sWAT of treated animals, which sustain the sympathetic tone that is crucial to the browning phenomenon (enhanced *β3-ar* expression). Also, linagliptin seems to activate PPAR-α as a pleiotropic effect. Following PPAR-α activation, PGC1α induces mitochondrial biogenesis, and PRDM16 orchestrates the unilocular adipocyte fashion towards a multilocular conformation (beige adipocyte) and maintains this new phenotype. All these critical thermogenic and browning mediators were induced by linagliptin more thoroughly in the HF-L group that continued to be exposed to excessive lipid intake during the treatment. Also, PPAR-α has *Ucp1* as a target gene, implying enhanced thermogenesis as UCP1 is its main effector, which was proved by the higher temperature and positive UCP1 immunostaining in linagliptin-treated animals.

The findings on sWAT of DIO mice after chronic administration of 30 mg/kg of linagliptin indicate that its benefits go beyond the glycemic homeostasis and the previously suggested effect in reducing hepatic steatosis [19]. Linagliptin has a predominant excretion through feces, allowing the administration to renal impaired patients without dose adjustment, differing from other gliptins [26, 27]. This property reassures the translational potential of the present findings as linagliptin is currently used as

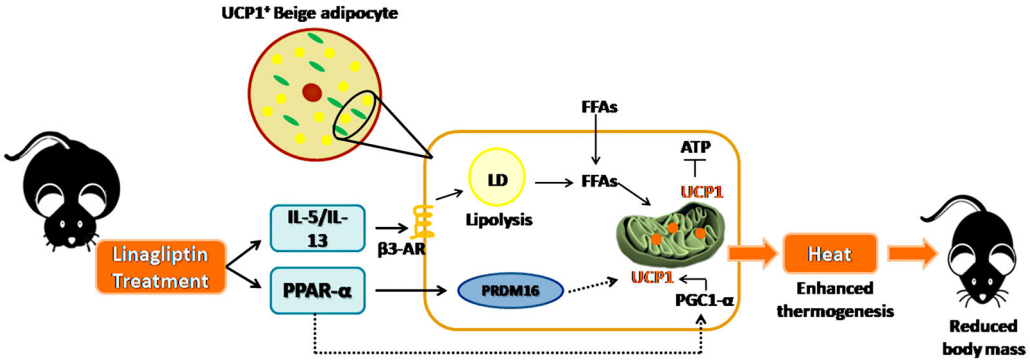

Fig. 6 Graphical abstract. Linagliptin yielded *Il-5* and *Il-13* expression, which correlates to a sustained sympathetic stimulation; and *Ppar-α*, which is linked to *Prdm16* and *Pgc1α* induction and the following mitochondrial biogenesis and favored *Ucp1* expression. This scenario induces the browning of the subcutaneous white adipose after the treatment, verified by positive UCP1 cells and high body temperature in diet-induced obese animals. These observations collaborated to the normalization of body mass

monotherapy or combined with other drugs in humans aiming at glycemic homeostasis, with potential cardio-renal benefits [46, 47]. However, it is essential to mention that more information about inflammatory pathways and eventual damage or injury to any organ might be investigated.

In conclusion, the proposed linagliptin treatment was able to reduce the adiposity index and ameliorate the sWAT structure in obese mice, parallel to the normalization of BM and high expression of thermogenic markers coupled with evidence of ILC2s activation in the sWAT and the alleviation of iBAT whitening. Treated animals had restoration of glucose tolerance and higher body temperature than their untreated counterparts. These results coupled with the presence of positive UCP1 beige cells in the sWAT of treated animals point to the activation of the browning cascade in the sWAT, and hence, linagliptin could induce the thermogenic pathway of the treated animals as a pleiotropic effect that can have translational potential.

Acknowledgements We thank Michele Soares and Aline Penna for their technical assistance.

Funding This study was financed in part by the Coordenação de Aperfeiçoamento de Pessoal de Nível Superior–Brasil (CAPES)—Finance Code 001 and supported by Fundação Carlos Chagas Filho de Amparo à Pesquisa do Rio de Janeiro (Faperj, Grant number 202.657/2018 for V.S.-M.).

Compliance with ethical standards

Conflict of interest The authors declare that they have no conflict of interest.

Ethical approval All applicable international, national, and/or institutional guidelines for the care and use of animals were followed. This work was approved by the local ethics committee under the number CEUA/022/2018.

Publisher's note: Springer Nature remains neutral with regard to jurisdictional claims in published maps and institutional affiliations.

References

1. A. Hruby, F.B. Hu, The epidemiology of obesity: a big picture. Pharmacoeconomics **33**(7), 673–689 (2015)
2. B. Gustafson, S. Hedjazifar, S. Gogg, A. Hammarstedt, U. Smith, Insulin resistance and impaired adipogenesis. Trends Endocrinol. Metab. **26**(4), 193–200 (2015)
3. B. Gustafson, U. Smith, Regulation of white adipogenesis and its relation to ectopic fat accumulation and cardiovascular risk. Atherosclerosis **241**(1), 27–35 (2015)
4. R.S. Ahima, Adipose tissue as an endocrine organ. Obes. (Silver Spring). **14**(Suppl 5), 242S–249S (2006)
5. A. Rodriguez, S. Ezquerro, L. Mendez-Gimenez, S. Becerril, G. Fruhbeck, Revisiting the adipocyte: a model for integration of cytokine signaling in the regulation of energy metabolism. Am. J. Physiol. Endocrinol. Metab. **309**(8), E691–E714 (2015)
6. J. Wu, P. Cohen, B.M. Spiegelman, Adaptive thermogenesis in adipocytes: is beige the new brown? Genes Dev. **27**(3), 234–250 (2013)
7. J. Nedergaard, B. Cannon, The browning of white adipose tissue: some burning issues. Cell Metab. **20**(3), 396–407 (2014)
8. K.A. Virtanen, M.E. Lidell, J. Orava, M. Heglind, R. Westergren, T. Niemi et al., Functional brown adipose tissue in healthy adults. N. Engl. J. Med. **360**(15), 1518–1525 (2009)
9. T.L. Rachid, A. Penna-de-Carvalho, I. Bringhenti, M.B. Aguila, C.A. Mandarim-de-Lacerda, V. Souza-Mello, Fenofibrate (PPARalpha agonist) induces beige cell formation in subcutaneous white adipose tissue from diet-induced male obese mice. Mol. Cell Endocrinol. **402**, 86–94 (2015)
10. T.L. Rachid, F.M. Silva-Veiga, F. Graus-Nunes, I. Bringhenti, C. A. Mandarim-de-Lacerda, V. Souza-Mello, Differential actions of PPAR-alpha and PPAR-beta/delta on beige adipocyte formation: a study in the subcutaneous white adipose tissue of obese male mice. PLoS ONE **13**(1), e0191365 (2018)
11. F. Graus-Nunes, T.L. Rachid, de Oliveira Santos, F., Barbosa-da-Silva, S., Souza-Mello, V., AT1 receptor antagonist induces thermogenic beige adipocytes in the inguinal white adipose tissue of obese mice. Endocrine **55**(3), 786–798 (2017).
12. H.Y. Kwan, J. Wu, T. Su, X.J. Chao, B. Liu, X. Fu et al., Cinnamon induces browning in subcutaneous adipocytes. Sci. Rep. **7** (1), 2447 (2017)
13. J.H. Choi, J.W. Yun, Chrysin induces brown fat-like phenotype and enhances lipid metabolism in 3T3-L1 adipocytes. Nutrition **32** (9), 1002–1010 (2016)
14. D. Lamers, S. Famulla, N. Wronkowitz, S. Hartwig, S. Lehr, D.M. Ouwens et al., Dipeptidyl peptidase 4 is a novel adipokine

potentially linking obesity to the metabolic syndrome. Diabetes **60** (7), 1917–1925 (2011)
15. H. Sell, M. Bluher, N. Kloting, R. Schlich, M. Willems, F. Ruppe et al., Adipose dipeptidyl peptidase-4 and obesity: correlation with insulin resistance and depot-specific release from adipose tissue in vivo and in vitro. Diabetes Care. **36**(12), 4083–4090 (2013)
16. V. Souza-Mello, B.M. Gregorio, F.S. Cardoso-de-Lemos, L. de Carvalho, M.B. Aguila, C.A. Mandarim-de-Lacerda, Comparative effects of telmisartan, sitagliptin and metformin alone or in combination on obesity, insulin resistance, and liver and pancreas remodelling in C57BL/6 mice fed on a very high-fat diet. Clin. Sci. (Lond.). **119**(6), 239–250 (2010)
17. F. Zhuge, Y. Ni, M. Nagashimada, N. Nagata, L. Xu, N. Mukaida et al., DPP-4 inhibition by linagliptin attenuates obesity-related inflammation and insulin resistance by regulating M1/M2 macrophage polarization. Diabetes **65**(10), 2966–2979 (2016)
18. N. Jeremic, P. Chaturvedi, S.C. Tyagi, Browning of white fat: novel insight into factors, mechanisms, and therapeutics. J. Cell Physiol. **232**(1), 61–68 (2017)
19. M. Kern, N. Kloting, H.G. Niessen, L. Thomas, D. Stiller, M. Mark et al., Linagliptin improves insulin sensitivity and hepatic steatosis in diet-induced obesity. PLoS ONE **7**(6), e38744 (2012)
20. P.G. Reeves, F.H. Nielsen, G.C. Fahey Jr., AIN-93 purified diets for laboratory rodents: final report of the American Institute of Nutrition ad hoc writing committee on the reformulation of the AIN-76A rodent diet. J. Nutr. **123**(11), 1939–1951 (1993)
21. A. Penna-de-Carvalho, F. Graus-Nunes, J. Rabelo-Andrade, C.A. Mandarim-de-Lacerda, V. Souza-Mello, Enhanced pan-peroxisome proliferator-activated receptor gene and protein expression in adipose tissue of diet-induced obese mice treated with telmisartan. Exp. Physiol. **99**(12), 1663–1678 (2014)
22. S.A. Tschanz, P.H. Burri, E.R. Weibel, A simple tool for stereological assessment of digital images: the STEPanizer. J. Microsc. **243**(1), 47–59 (2011)
23. C.A. Mandarim-De-Lacerda, Stereological tools in biomedical research. An. Acad. Bras. Cienc. **75**(4), 469–486 (2003)
24. M.T. Davisson, Rules and guidelines for nomenclature of mouse genes. International Committee on Standardized Genetic Nomenclature for Mice. Gene **147**, 157–160 (1994)
25. M. Eckhardt, E. Langkopf, M. Mark, M. Tadayyon, L. Thomas, H. Nar et al., 8-(3-(R)-aminopiperidin-1-yl)-7-but-2-ynyl-3-methyl-1-(4-methyl-quinazolin-2-ylme thyl)-3,7-dihydropurine-2,6-dione (BI 1356), a highly potent, selective, long-acting, and orally bioavailable DPP-4 inhibitor for the treatment of type 2 diabetes. J. Med Chem. **50**(26), 6450–6453 (2007)
26. J.B. McGill, Linagliptin for type 2 diabetes mellitus: a review of the pivotal clinical trials. Ther. Adv. Endocrinol. Metab. **3**(4), 113–124 (2012)
27. S. Del Prato, A.H. Barnett, H. Huisman, D. Neubacher, H.J. Woerle, K.A. Dugi, Effect of linagliptin monotherapy on glycaemic control and markers of beta-cell function in patients with inadequately controlled type 2 diabetes: a randomized controlled trial. Diabetes Obes. Metab. **13**(3), 258–267 (2011)
28. I. Shimizu, K. Walsh, The whitening of brown fat and its implications for weight management in obesity. Curr. Obes. Rep. **4**(2), 224–229 (2015)
29. D. Duteil, M. Tosic, F. Lausecker, H.Z. Nenseth, J.M. Muller, S. Urban et al., Lsd1 ablation triggers metabolic reprogramming of brown adipose tissue. Cell Rep. **17**(4), 1008–1021 (2016)
30. J.R. Arch, D. Hislop, S.J. Wang, J.R. Speakman, Some mathematical and technical issues in the measurement and interpretation of open-circuit indirect calorimetry in small animals. Int J. Obes. **30**(9), 1322–1331 (2006)
31. T.C.L. Bargut, V. Souza-Mello, M.B. Aguila, C.A. Mandarim-de-Lacerda, Browning of white adipose tissue: lessons from experimental models. Horm. Mol. Biol. Clin. Investig. (2017). https://doi.org/10.1515/hmbci-2016-0051
32. D. Ricquier, UCP1, the mitochondrial uncoupling protein of brown adipocyte: a personal contribution and a historical perspective. Biochimie **134**, 3–8 (2017)
33. D. Ricquier, B. Miroux, M. Larose, A.M. Cassard-Doulcier, F. Bouillaud, Endocrine regulation of uncoupling proteins and energy expenditure. Int J. Obes. Relat. Metab. Disord. **24**(Suppl 2), S86–S88 (2000)
34. B.M. Spiegelman, Banting Lecture 2012: regulation of adipogenesis: toward new therapeutics for metabolic disease. Diabetes **62**(6), 1774–1782 (2013)
35. A.V. Kalinovich, J.M. de Jong, B. Cannon, J. Nedergaard, UCP1 in adipose tissues: two steps to full browning. Biochimie **134**, 127–137 (2017)
36. M. Jimenez, G. Barbatelli, R. Allevi, S. Cinti, J. Seydoux, J.P. Giacobino et al., Beta 3-adrenoceptor knockout in C57BL/6J mice depresses the occurrence of brown adipocytes in white fat. Eur. J. Biochem. **270**(4), 699–705 (2003)
37. O. Braissant, F. Foufelle, C. Scotto, M. Dauca, W. Wahli, Differential expression of peroxisome proliferator-activated receptors (PPARs): tissue distribution of PPAR-alpha, -beta, and -gamma in the adult rat. Endocrinology **137**(1), 354–366 (1996)
38. F.M.S. Veiga, F. Graus-Nunes, T.L. Rachid, A.B. Barreto, C.A. Mandarim-de-Lacerda, V. Souza-Mello, Anti-obesogenic effects of WY14643 (PPAR-alpha agonist): hepatic mitochondrial enhancement and suppressed lipogenic pathway in diet-induced obese mice. Biochimie **140**, 106–116 (2017)
39. D. Namgaladze, S. Lips, T.J. Leiker, R.C. Murphy, K. Ekroos, N. Ferreiros et al., Inhibition of macrophage fatty acid beta-oxidation exacerbates palmitate-induced inflammatory and endoplasmic reticulum stress responses. Diabetologia **57**(5), 1067–1077 (2014)
40. D.A. Chistiakov, M.C. Killingsworth, V.A. Myasoedova, A.N. Orekhov, Y.V. Bobryshev, CD68/macrosialin: not just a histochemical marker. Lab. Invest. **97**(1), 4–13 (2017)
41. J. Chylikova, J. Dvorackova, K. Cizkova, H. Lacey, V. Kamarad, Macrophages of the subcutaneous and omental fatty tissue in obese patients: Immunohistochemical phenotyping of M2 subtypes in relation to type 2 diabetes. Biomed. Pap. Med. Fac. Univ. Palacky Olomouc Czech Repub (2019). https://doi.org/10.5507/bp.2019.011
42. P. Seale, B. Bjork, W. Yang, S. Kajimura, S. Chin, S. Kuang et al., PRDM16 controls a brown fat/skeletal muscle switch. Nature **454**(7207), 961–967 (2008)
43. Y. Qiu, K.D. Nguyen, J.I. Odegaard, X. Cui, X. Tian, R.M. Locksley et al., Eosinophils and type 2 cytokine signaling in macrophages orchestrate development of functional beige fat. Cell **157**(6), 1292–1308 (2014)
44. M.W. Lee, J.I. Odegaard, L. Mukundan, Y. Qiu, A.B. Molofsky, J.C. Nussbaum et al., Activated type 2 innate lymphoid cells regulate beige fat biogenesis. Cell **160**(1–2), 74–87 (2015)
45. X. Ding, Y. Luo, X. Zhang, H. Zheng, X. Yang, M. Liu, IL-33-driven ILC2/eosinophil axis in fat is induced by sympathetic tone and suppressed by obesity. J. Endocrinol. **231**(1), 35–48 (2016)
46. T. Forst, B. Uhlig-Laske, A. Ring, U. Graefe-Mody, C. Friedrich, K. Herbach et al., Linagliptin (BI 1356), a potent and selective DPP-4 inhibitor, is safe and efficacious in combination with metformin in patients with inadequately controlled Type 2 diabetes. Diabet. Med. **27**(12), 1409–1419 (2010)
47. R. Kawamori, M. Haneda, K. Suzaki, G. Cheng, K. Shiki, Y. Miyamoto, et al., Empagliflozin as add-on to linagliptin in a fixed-dose combination in Japanese patients with type 2 diabetes: glycaemic efficacy and safety profile in a 52-week, randomized, placebo-controlled trial. Diabetes Obes. Metab. **20**(9), 2200–2209 (2018)